Dyes and Pigments 94 (2012) 136–142

Contents lists available at SciVerse ScienceDirect

Dyes and Pigments

journal homepage: www.elsevier.com/locate/dyepig

Synthesis and properties of novel spirobifluorene-cored dendrimers

Huicai Ren, Qian Tao, Zhanxian Gao, Di Liu*

School of Chemistry, Dalian University of Technology, 2 Linggong Road, Dalian 116024, China

ARTICLE INFO

Article history:
Received 24 October 2011
Received in revised form
12 December 2011
Accepted 15 December 2011
Available online 21 December 2011

Keywords:
Dendrimer
Polyphenylene dendron
Spirobifluorene
Amorphous
High glass transition temperature

ABSTRACT

Two novel spirobifluorene-cored dendrimers containing polyphenylene dendrons with the carbazole (**spiro-Cz**) and cyano surface groups (**spiro-CN**) were synthesized and characterized. Both the dendrimers show good solubility in common organic solvents. **Spiro-Cz** is amorphous even when it is obtained directly from organic solvents and an extremely high glass transition temperature of 332 °C is detected. These dendrimers can be reversibly oxidized and reduced in electrochemical measurements. They are blue fluorescent with small red-shift in solid film absorption and fluorescence spectra. These advantageous merits are suggested to benefit from the combined contribution from the spirobifluorene core and the bulky polyphenylene dendrons. They were used as emitting layer to fabricate organic light-emitting diodes (OLEDs). Deep-blue electroluminescence was obtained for both dendrimers devices.

1. Introduction

For the past decades, polyfluorene and its derivatives have been known as the most promising blue light-emitting materials due to their high fluorescent quantum yields and excellent chemical and thermal stability [1,2]. However, the rigid and planar biphenyl structure of these compounds always leads to the reduction of color purity and stability of the devices due to the tendency to aggregate and crystallize in the solid state or excimer formation [3–5]. Because of these drawbacks, there has been a considerable interest in 9,9′-spirobifluorene that consists of two more or less extended π-systems with identical or different functions (emission, charge transport) via a sp^3-hybridized carbon atom at the spiro center [6–9]. The rings of the connected bifluorene entities are arranged orthogonally in the spiro segment. This high steric and rigid structure not only efficiently suppresses the excimer formation and molecular interactions between the π-systems, but also results in a high stability of the amorphous state, that is, a high glass transition temperature (T_g) which is an important factor to improve the durability of organic light-emitting diodes (OLEDs). Recently, several spirobifluorene-based compounds with high T_g have been successfully synthesized: fully spiro-configured terfluorene with a T_g up to 296 °C [10], spirobifluorene-linked bisanthracene with a T_g up to 223 °C [11], and spiro-linked oligothiophene with a T_g up to 205 °C [12]. Furthermore, the chemical modification could be easily achieved at the 2,2′,7,7′-positions of spirobifluorene.

On the other hand, a new class of functional organic material, dendrimer, has been extensively applied as active materials for optoelectronic devices such as organic light-emitting diodes (OLEDs) [13–17] and solar cells [13,18]. The well-defined three-dimensional dendritic structures can greatly improve the solubility and film forming ability and make these materials show high thermal and chemical stabilities. In addition, the emissive core, dendrons and surface groups of dendrimers can be individually modified to optimize the overall properties including light-emitting wavelength and efficiency, the charge-transporting ability and the solubility. This is the advantageous merit of dendrimers over the traditional small molecules and polymers based optoelectronic materials.

Our interest is to take advantages of spirobifluorene skeleton to develop novel spirobifluorene-cored dendrimers for optoelectronic application. The bulky polyphenylene groups (Müllen type dendrons) [19] are selected and incorporated at the 2,2′,7,7′-positions of the spirobifluorene core in order to further enhance the non-planar conformation of the resultant molecules and consequently tune the stability, solubility and so on. 3,6-Di-tert-butylcarbazole or cyano groups are grafted to the periphery of dendrons with the aim to tune the electrochemical redox behavior and thus the charge injecting or transporting ability of the target dendrimers, respectively. The dendrimers designed in such a way are expected to have three-dimensional non-planar conformation and to show remarkable thermal and morphological stabilities. Herein, we report the

* Corresponding author. Fax: +86 411 84986233.
E-mail address: liudi@dlut.edu.cn (D. Liu).

0143-7208/$ – see front matter © 2011 Elsevier Ltd. All rights reserved.
doi:10.1016/j.dyepig.2011.12.005

synthesis and characterization of these novel spirobifluorene-cored dendrimers, **spiro-Cz** and **spiro-CN** (Scheme 1). The optical, thermal and electrochemical properties of these dendrimers are investigated as well. These dendrimers were also used as emitting layer to fabricate OLEDs and their electroluminescent properties are studied.

2. Experimental

2.1. Materials and instruments

All the reagents are of analytical grade and used as received from commercial sources without further purification. ^{1}H NMR spectra were recorded on a Varian INOVA spectrometer (400 MHz). Chemical shifts were referenced to TMS. Mass spectra were recorded on a Micromass Q-Tof (Micromass, Wythenshawe, UK) mass spectrometer for ESI-MS and a Micro MX (Micromass) Mass Spectrometer for MALDI-TOF-MS. Thermogravimetric analyses (TGA) were carried out using a Perkin–Elmer thermogravimeter (Model TGA 7) under a dry nitrogen gas flow by heating samples from room temperature to 600 °C at a rate of 10 °C min^{-1}. The differential scanning calorimetry (DSC) was performed on a NETZSCH DSC 204 at a scan rate of 10 °C min^{-1}. The fluorescence and absorption spectra were measured on a Perkin–Elmer LS55 fluorescence spectrometer and a Perkin–Elmer Lambda 35 UV–Vis spectraphotometer, respectively. The relative fluorescent quantum yields (Φ_F) of these dendrimers were measured in dilute cyclohexane solutions using 9,10-diphenylanthracene as the standard ($\Phi_F = 90\%$ in cyclohexane).

2.2. Electrochemistry

Cyclic voltammetry (CV) measurements were performed using a conventional three-electrode cell with a glassy carbon working electrode, a platinum wire counter electrode, and an Ag/AgCl reference electrode on a computer-controlled BAS 100W electrochemical analyzer at room temperature. Positive values are typically measured in CH_2Cl_2 and negative values in THF with Bu_4NPF_6 (0.1 M) as the supporting electrolyte. The redox potentials were obtained at the scan rate of 100 mV/s, and with ferrocene/ferrocenium (Fc/Fc^+) as an internal standard of the redox system. The highest occupied molecular orbital (HOMO) and the lowest unoccupied molecular orbital (LUMO) energy levels of the studied dendrimers were determined from the onset potential of the first oxidation (E^{ox}_{onset}) and first reduction (E^{red}_{onset}) wave, based on the reference energy level of Fc/Fc^+ (4.8 eV below the vacuum level) [20].

2.3. Synthesis

2.3.1. Synthesis of 4, 4′-Dibromobenzoin (**1**)

A 250 ml round-bottom flask was charged with VB1 (5 g, 20 mmol) dissolved in distilled water (5 ml) and ethanol (100 ml). The mixture was cooled by an ice-salt bath. When the temperature was below zero, a 10% NaOH solution in distilled water was added dropwisely until the pH reached to 9. Then 4-bromobenzaldehyde (20 g, 108 mmol) was added, and the mixture was kept at 65 °C and stirred for 12 h. The solution was cooled and the precipitate was filtered off, washed with water and ethanol. The crude product was a mixture of benzoin and benzil. Crystallization from ethanol gave pure compound **1** (11 g, 55%) as white crystals. mp: 92–93 °C (lit. [21]: 94–96.5 °C).

2.3.2. Synthesis of 4, 4′-Dibromobenzil (**2**)

A solution of compound **1** (500 mg, 1.35 mmol), NH_4NO_3 (135 mg, 1.69 mmol), and $Cu(OAc)_2 \cdot H_2O$ (31.4 mg, 0.17 mmol) in acetic acid (5.5 ml) was stirred and refluxed for 2 h. Upon cooling to room temperature, a precipitate was formed. Filtration followed by washing with water and ethanol gave pure **8** (409 mg, 84.5%) as yellow crystal. mp: 230–232 °C. IR (KBr, cm^{-1}): 3090 (=C–H stretch), 1664 (C=O stretch), 1586 (C=C stretch). ^{1}H NMR (400 MHz, $CDCl_3$) δ (ppm): 7.83 (d, $J = 8.4$ Hz, 4H, ArH), 7.67 (d, $J = 8.4$ Hz, 4H, ArH). ESI-MS (m/z): calcd. for $C_{14}H_8Br_2O_2$ 368.02; found 368.0 ($[M]^+$).

2.3.3. Synthesis of 4, 4′-Di(3,6-di-tert-butylcarbazol-9-yl) benzil (3)

A solution of compound **2** (2 g, 5.4 mmol), 3,6-Di-*tert*-carbazole (3.34 g, 12 mmol), CuI (207 mg, 1.1 mmol), anhydrous K_2CO_3 (2.25 g, 16 mmol) and 18-crown-6 (537 mg, 2 mmol) in nitrobenzene (35 ml) was stirred and refluxed for 5 h under nitrogen. Upon cooling, the precipitate was filtered. The solvent was removed under reduced pressure, and the crude product was purified by column chromatography on silica gel to afford 2.2 g (55% in yield) **3** as pale yellow solid.

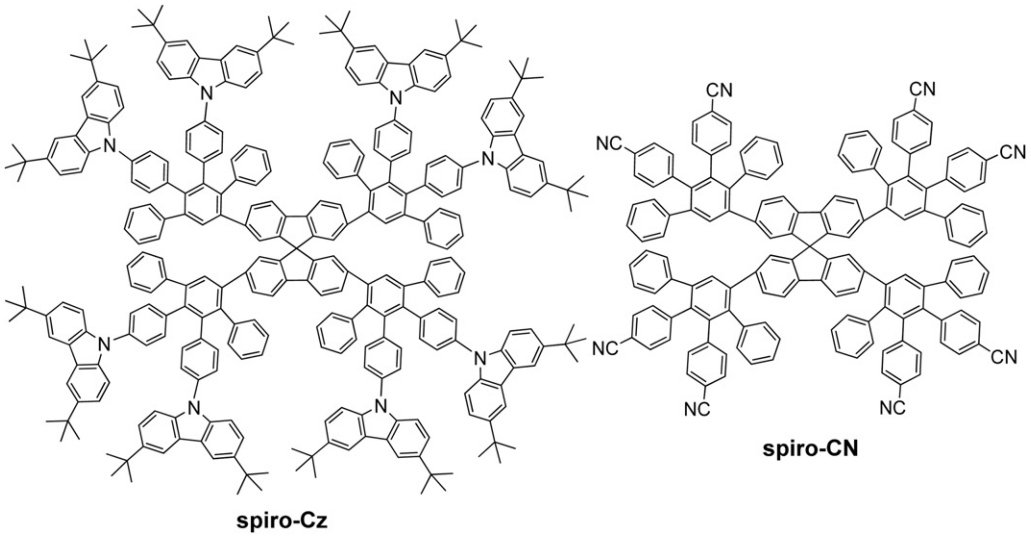

Scheme 1. Chemical structures of the dendrimers in present study.

^{1}H NMR (400 MHz, $CDCl_3$) δ (ppm): 8.28 (d, J = 8.4 Hz, 4H), 8.14 (s, 4H), 7.80 (d, J = 8.4 Hz, 4H), 7.50 (s, 8H), 1.47 (s, 36H). ESI-MS (m/z): calcd. for $C_{54}H_{56}N_2O_2$, 764.4; found, 764.5 ($[M]^+$)

*2.3.4. Synthesis of 3,4-Bis[4,4′-Di(3,6-di-tert-butylcarbazol-9-yl) phenyl]2,5-diphenyl-cyclopenta-2,4-di-enone (**Cp-Cz**)*

A 25 ml round-bottom flask was charged with compound **3** (800 mg, 1.05 mmol), 1, 3-diphenylacetone (219.6 mg, 1.05 mmol), anhydrous KOH (58.8 mg, 1.16 mmol) and absolute ethyl alcohol (10 ml). The mixture was stirring for 30 min under reflux. Removing of the solvent under reduced pressure gave the crude product, purification of which by column chromatography on silica gel yielded pure **Cp-Cz** (550 mg, 56%) as a brown solid.

^{1}H NMR (400 MHz, $CDCl_3$) δ (ppm): 8.13 (s, 4H), 7.49 (d, J = 8 Hz, 4H), 7.42 (d, J = 8.8 Hz, 4H), 7.36 (m, 14H), 7.23 (d, J = 8 Hz, 4H), 1.47 (s, 36H). ESI-MS (m/z): calcd. for $C_{69}H_{66}N_2O$, 939.2751; found, 939.4039 ($[M]^+$).

*2.3.5. Synthesis of 3,4-bis-(4-bromophenyl)-2,5-diphenyl-cyclopentadienone (**Cp-Br**)*

A 25 ml round-bottom flask was charged with compound **2** (1.2 g, 3.26 mmol), 1, 3-diphenylacetone (600 mg, 3.26 mmol), anhydrous KOH (200 mg, 3.59 mmol) and absolute ethyl alcohol (15 ml). The mixture was stirring for 30 min under reflux. Removing of the solvent under reduced pressure gave the crude product, purification of which by column chromatography on silica gel yielded pure compound 3 (1.5 g, 85%) as a dark brown solid. ^{1}H NMR (400 MHz, $CDCl_3$) δ (ppm): 6.77 (dd, J = 2.1, 8.7 Hz, 4H, ArH), 7.1–7.3 (m, 10H, ArH), 7.34 (dd, J = 2.1, 8.7 Hz, 4H, ArH). ESI-MS (m/z): calcd. for $C_{29}H_{18}Br_2O$ 542.2606; found 542.2610 ($[M]^+$).

*2.3.6. Synthesis of 3,4-bis-(4-cyanophenyl)-2,5-diphenylcyclopenta-dienone (**Cp-CN**)*

A 25 ml round-bottom flask was charged with compound **Cp-Br** (500 mg, 0.92 mmol), $K_4Fe(CN)_6$ (156 mg, 0.37 mmol), $Pd(OAc)_2$ (2 mg, 0.01 mmol), P(t-Bu)$_3$ (0.08 ml, 0.03 mmol) and Na_2CO_3 (39 mg, 0.37 mmol) and NMP (10 ml). The mixture was stirring for 7 h at 140 °C under nitrogen. Removing of the solvent under reduced pressure gave the crude product, purification of which by column chromatography on silica gel yielded pure compound **Cp-CN (**200 mg, 50%**)** as a dark solid. ^{1}H NMR (400 MHz, $CDCl_3$) δ (ppm): 6.95 (d, J = 8.6 Hz, 4H, ArH), 7.12–7.05 (m, 4H, ArH), 7.28–7.20 (m, 6H, ArH), 7.45 (d, J = 8.6 Hz, 4H, ArH). ESI-MS (m/z): calcd. for $C_{31}H_{18}N_2O$ 434.1419; found 434.1423 ($[M]^+$).

*2.3.7. Synthesis of 2,2′,7,7′-tetra((trimethylsily) ethyny)l-9,9′-spirobifluorene (**4**)*

2,2′,7,7′-Tetrabromo-9,9′-spirobifluorene (2 g, 3.16 mmol), $Pd(PPh_3)_2Cl_2$ (266 mg, 0.379 mmol), CuI (301 mg, 1.58 mmol), and PPh_3 (414 mg, 1.58 mmol) were dissoved in 20 ml diethylamine. Then trimethylsilylacetylene (2.7 mL, 19 mmol) was added via a syringe. The reaction mixture was brought to reflux overnight and then cooled down to room temperature. The solvent was removed in vacuum, and the crude product was purified by chromatography on silica gel to obtain white solid product (1.87 g, 84% yield). ^{1}H NMR (400 MHz, $CDCl_3$) δ (ppm): 0.16 (s, 36H, CH_3), 6.77 (s, 4H, ArH), 7.49 (dd, J = 1.2, 7.6 Hz, 4H, ArH), 7.74 (d, J = 8 Hz, 4H, ArH). ESI-MS (m/z): calcd. for $C_{45}H_{48}Si_4$ 700.2833; found 700.2850 ($[M]^+$).

*2.3.8. Synthesis of 2,2′,7,7′-tetraethynyl-9,9′-spirobifluorene (**5**)*

NaOH (220 mg, 20 mmol) was dissolved in 5 mL of CH_3OH, then added to a solution of compound **4** (1.4 g, 2 mmol) in 20 mL of CH_2Cl_2, and then stirred over night at room temperature. The reaction mixture was washed with water, and the aqueous phase was extracted with CH_2Cl_2 and then dried over anhydrous $MgSO_4$. The solvent was removed under reduced pressure. The crude product was purified by chromatography on silica gel to obtain yellow solid product (0.66 g, 80% yield). ^{1}H NMR (400 MHz, $CDCl_3$) δ (ppm): 3.01(s, 4H, C^CH), 6.83(s, 4H, ArH), 7.54(dd, J = 1.2, 7.6 Hz, 4H, ArH), 7.79(d, J = 8 Hz, 4H, ArH). ESI-MS (m/z): calcd. for $C_{33}H_{16}$ 412.1252; found 412.1263 ($[M]^+$).

2.3.9. General procedure for synthesis of the target dendrimers

A mixture of compound **5** (0.15 mmol) and the corresponding cyclopentadienone (6 equiv) in *o*-xylene (15 ml) was stirred at 140 °C for 12 h under nitrogen. The solvent was removed under reduced pressure. The crude product was purified by column chromatography on silica gel and then recrystallized from chloroform and methanol to afford the target dendrimers.

spiro-Cz: yield 75% as a white powder. ^{1}H NMR (400 MHz, $CDCl_3$) δ (ppm): 8.08 (d, J = 2 Hz, 16H, ArH), 7.62 (s, 4H, ArH), 7.46 (d, J = 7.6 Hz, 4H, ArH), 7.31–6.99(m, 88 H, ArH), 6.82–6.68(m, 24H,

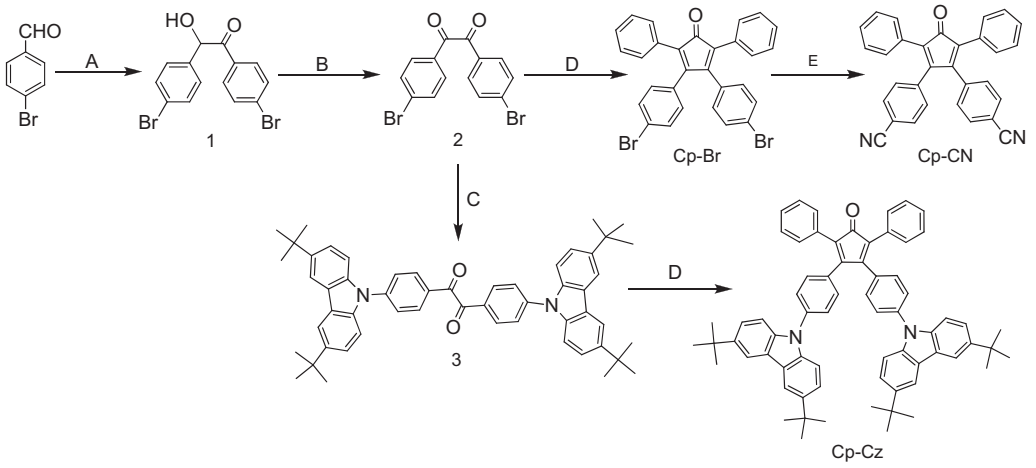

(A): VB1, NaOH, H_2O, EtOH; (B): NH_4NO_3, $Cu(OAc)_2$; (C): CuI, 18-crown-6, K_2CO_3, reflux, nitrobenzene; (D): KOH, EtOH, 1,3-diphenylacetone, reflux; (E): $K_4Fe(CN)_6$, $Pd(OAc)_2$, P(t-Bu)$_3$, Na_2CO_3, NMP.

Scheme 2. Synthetic routes of the important intermediate **Cp-Cz** and **Cp-CN**.

ArH), 1.40 (s, 144H, CH_3). MALDI-TOF-MS: (m/z): calcd for $C_{305}H_{280}N_8$ 4054.2156; found 4056.1604 ($[M]^+$).

spiro-CN: yield 80% as a white powder. ^{1}H NMR (400 MHz, $CDCl_3$) δ (ppm): 7.45 (s, 4H, ArH), 7.36 (d, J = 8 Hz, 4H, ArH), 7.24 (d, J = 7.6 Hz, 8H, ArH), 7.19–7.15 (m, 20H, ArH), 7.04–7.02 (m, 8H, ArH), 6.93–6.90 (dd, J = 1.2, 8 Hz, 4H, ArH), 6.88 (d, J = 8 Hz, 8H, ArH), 6.78 (d, J = 8.4 Hz, 8H, ArH), 6.61–6.48 (m, 24H, ArH). MALDI-TOF-MS: (m/z): calcd for $C_{153}H_{88}N_8$ 2036.7132; found 2036.7667 ($[M]^+$).

2.4. OLED fabrication and measurements

The light-emitting devices have a configuration of ITO/PEDOT:PSS (40 nm)/dendrimer (40 nm)/TPBI (30 nm)/LiF (1 nm)/Al (100 nm). The patterned ITO substrates were cleaned by successive ultrasonications in detergent, deionized water, ethanol, and chloroform, followed by treatment with UV–ozone. PEDOT:PSS (Bayer AG) was spin-coated on pretreated ITO substrate from aqueous dispersion and baked at 120 °C for 1 h. Subsequently the dendrimer layer was deposited on PEDOT:PSS film by spin-coating the dendrimer solutions in chlorobenzene, the thickness of which was controlled as 40 nm by tuning the solution concentration and spin rate. Then a thin layer of TPBI was vacuum deposited on top of dendrimer layer, followed by vacuum deposition of LiF (1 nm) and Al (100 nm) as cathode. The emitting area of each pixel is determined by overlapping of the two electrodes as 9 mm^2. The EL spectra, CIE coordinates, and current-voltage-luminance characteristics were measured with computer-controlled Spectrascan PR 705 photometer and a Keithley 236 source-measure-unit. All the measurements were carried out at room temperature under ambient conditions.

3. Results and discussion

3.1. Synthesis

The target demdrimers **spiro-Cz** and **spiro-CN** were synthesized through the typical Diels–Alder cycloaddition of the functionalized tetraphenyl-cyclopentedieneone (**Cp-Cz** and **Cp-CN**) to a spirobifluorene core containing four terminal ethynyl groups at the 2,2′,7,7′-positions (compound **5**). The important building blocks, **Cp-Cz** and **Cp-CN**, were obtained conveniently from 4-bromobenzaldehyde as the starting material through the route shown in Scheme 2. Both dendrimers were prepared in the divergent way (Scheme 3) from compound **5**, which was involved 2,2′,7,7′-tetrabromo-9,9′-spirobifluorene by treatment with trimethylsilylacetylene, followed by deprotection. The dendrimers are readily soluble in common organic solvents such as dichloromethane, chloroform, or toluene and were easily purified by column chromatograph. Characterization by MALDI-TOF mass spectrometry and ^{1}H NMR spectroscopy confirmed their chemical structures.

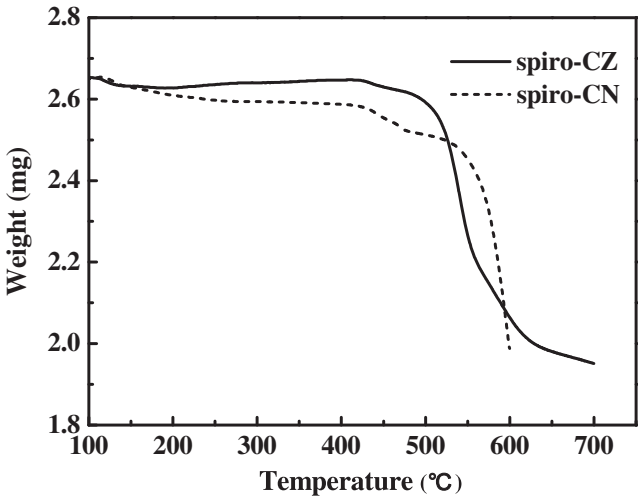

Fig. 1. TGA thermograms for dendrimers **spiro-Cz** and **spiro-CN**.

3.2. Thermal properties

The thermal properties of the spirobifluorene-cored dendrimers were investigated by thermogravimetric analysis (TGA) and differential scanning calorimetry (DSC). Both TGA and DSC measurements were carried out in nitrogen atmosphere at a heating rate of 10 °C min^{-1}. As shown in Fig. 1, both **spiro-Cz** and **spiro-CN** start to decompose at a high temperature up to 480 °C, indicating that such dendron functionalized materials have excellent thermal stability, which is an essential merit for fabricating stable optoelectronic devices. It should be noted that **spiro-CN** started to show a tiny weight loss at lower temperature than **spiro-Cz**, and then exhibited an obvious weight loss at a higher temperature, indicating **spiro-Cz** may possess higher thermal stability than **spiro-CN**. This should benefit from the extra contribution from carbazole groups that is characterized by excellent thermal and chemical stabilities. The phase transition behaviors of these dendrimers were investigated by means of DSC measurements. The DSC trace for **spiro-Cz** is shown in Fig. 2. When a dry powder of **spiro-Cz** obtained directly from organic solvents was heated at a rate of 10 °C min^{-1}, a typical endothermic process was detected at 332 °C, which is ascribed to the glass transition temperature (T_g) of this dendrimer. With further increasing temperature, an exothermic transition was observed at 372 °C, which corresponds to the crystallization of the dendrimer. No further change was

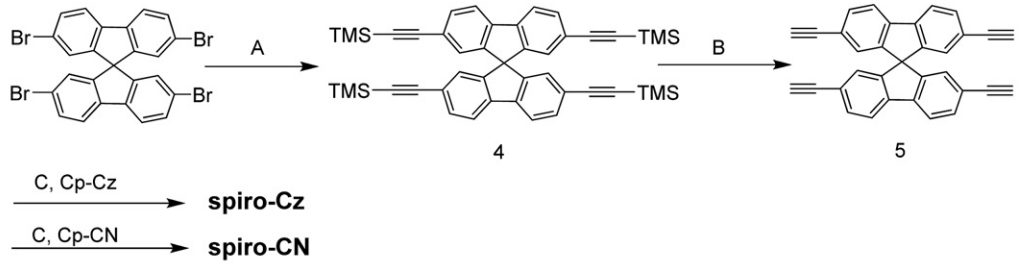

(A): $Pd(PPh_3)_2Cl_2$, CuI, PPh_3, trimethylsilylacetylene; (B):NaOH, CH_3OH, CH_2Cl_2; (D): *o*-xylene, 12h, reflux

Scheme 3. Synthetic routes of the dendrimers.

detected before 450 °C. The detection of T_g in the first heating run indicates that the dendrimer **spiro-Cz** is naturally amorphous even when it was obtained from organic solvents. It should be noted that such a T_g of 332 °C is remarkably high for organic molecules. Such a high T_g of 332 °C indicates that dendrimer **spiro-Cz** has extra stable amorphous state. For dendrimer **spiro-CN**, no glass transition or other phase change was observed when it was heated to 450 °C. We attribute the excellent thermal and amorphous stabilities of dendrimer **spiro-Cz** to the contribution from both the bulk dendritic polyphenylenes and the tetrahedral structure of spirobifluorene. Such a high T_g and high decomposition temperature determine that the spirobifluorene-based dendrimers would be desirable especially for high-temperature device applications.

3.3. Optical properties

The absorption and fluorescence spectra of these dendrimers were measured in dichloromethane solution as well as in solid film on quartz substrates. The spectra are shown in Fig. 3. In CH_2Cl_2 solutions, the absorption bands between 200 and 300 nm are from the benzene units while the weak absorption between 300 and 340 nm is ascribed to the π-π^* transition of the molecular skeleton. One additional absorption peak at 345 nm was only observed for **spiro-Cz**, which should be assigned to the transition absorption of carbazole units. For both dendrimers, the absorption spectra in films are nearly identical with the spectra in solutions, suggesting that there is minimal intermolecular interaction in thin films at the ground state. Upon photoexcitation at 330 nm, both dendrimers emit deep-blue fluorescence in dilute solutions with the emission maxima at 396 and 391 nm for **spiro-Cz** and **spiro-CN**, respectively. In solid state, only small red-shift of 5 nm were observed for the two dendrimers. These observations suggest that the orthogonal structure of spirobifluorene and the bulky polyphenylene dendrons efficiently suppress molecular interactions and excimer formation, which are frequently observed in solid state. The fluorescent quantum yields (Φ_F) of **spiro-Cz** and **spiro-CN** are determined as ca. 0.50 and 0.46 in dilute cyclohexane solutions, respectively, relative to 9, 10-diphenylanthracene in cyclohexane (Φ_F = 0.90) [22] as a standard.

3.4. Electrochemical properties

The electrochemical behavior of **spiro-Cz** and **spiro-CN** was investigated by cyclic voltammetry method in a nitrogen atmosphere. As shown in Fig. 4, during the anodic scan in CH_2Cl_2 solutions, reversible oxidation waves were observed with the onset potentials at 0.73 V and 1.1 V (vs. Fc/Fc^+) for **spiro-Cz** and **spiro-CN**, respectively. Upon the cathodic sweep in THF, a reversible reduction was detected with the onset potential at −2.3 V (vs. Fc/Fc^+) only for **spiro-CN**, while no reduction signal was observed for **spiro-Cz** within the detected potential range. Distinctively, the

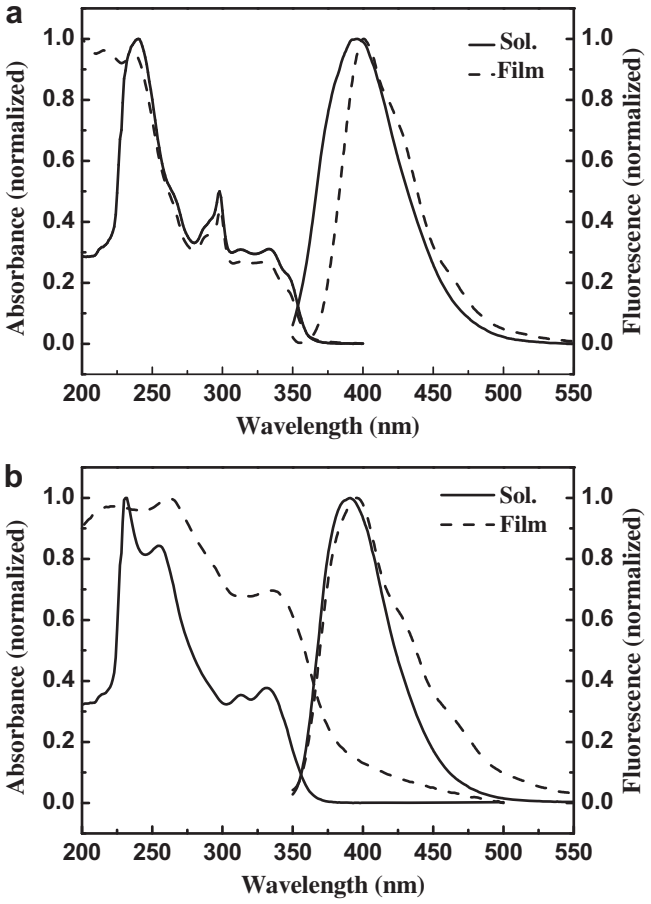

Fig. 3. Absorption and fluorescence spectra of a) **spiro-Cz** and b) **spiro-CN** in CH_2Cl_2 solutions (1×10^{-5} mol L^{-1}) and solid films (40 nm thick).

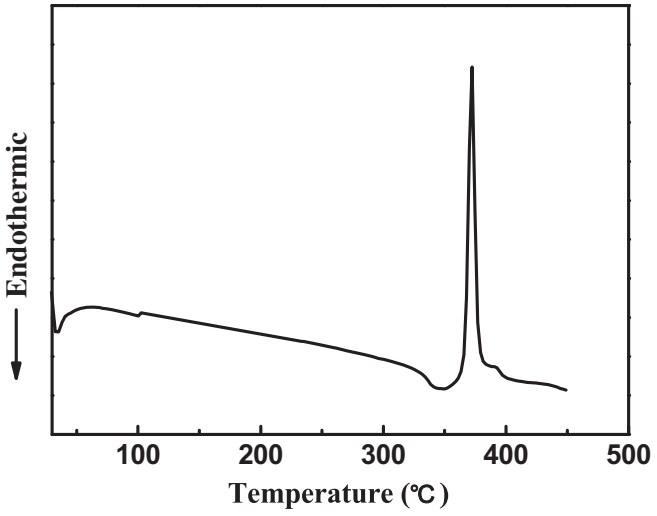

Fig. 2. DSC thermogram of **spiro-Cz** in the first heating cycle.

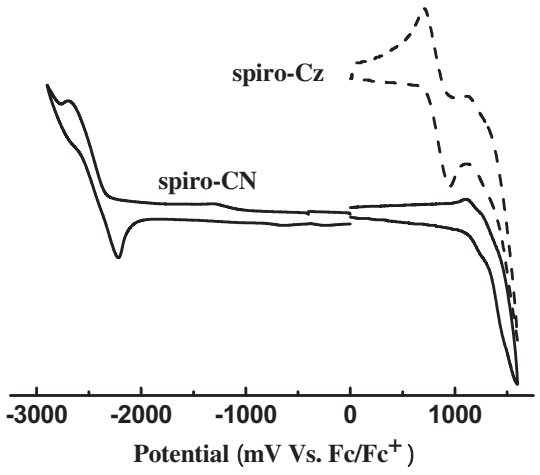

Fig. 4. Cyclic voltammograms of the studied dendrimers.

Tabel 1
EL performance data for dendrimers **spiro-Cz** and **spiro-CN** based OLEDs.

Dendrimer	V_{on} (V)	J_{max} (mA/cm^2)[a]	L_{max} (cd/m^2)[a]	η_{max} (cd/A)
Spiro-Cz	6	302 (14)	287 (13)	0.35
Spiro-CN	6	277 (11)	197 (11)	0.47

[a] Values in parentheses are the voltages at which they were obtained.

oxidation of **spiro-Cz** occurs at less positive potential if compared with **spiro-CN**. This should be because of the peripheral carbazole groups is electron-donating and make the corresponding dendrimer molecules much easier to be oxidized. The reversible reductive or oxidative behavior indicates that the dendrimers could be applied as hole- or electron- transporter in optoelectronic devices. The HOMO and LUMO energy levels were estimated from the onset potential of the first oxidation (E^{ox}_{onset}) and reduction (E^{red}_{onset}) waves, respectively, by using the following equations: HOMO (eV) $= -e(E^{ox}_{onset} + 4.8\ V)$, LUMO (eV) $= -e(E^{red}_{onset} + 4.8\ V)$, based on the energy level of the ferrocene reference (4.8 eV below the vacuum level) [20]. The HOMO energy levels for **spiro-Cz** and **spiro-CN** are determined as −5.53 and −5.9 eV, respectively. The LUMO energy level for **spiro-CN** is −2.5 eV and the electrochemical energy band gap is 3.4 eV. Since no reduction process was detected for **spiro-Cz**, its LUMO value was estimated as −2.11 eV by using the optical band gap of 3.42 eV that is determined by absorption edge technique [23]. The wide band gaps and proper HOMO and LUMO levels as well as their good solubility make these dendrimers promising materials to act as host in solution-processed optoelectronic devices such as OLEDs.

3.5. Electroluminescence properties

In order to evaluate the electroluminescence properties of these spirobifluorene-cored dendrimers, they were used as the non-doped emitting layer to fabricate OLEDs. The OLEDs have the configuration of ITO/PEDOT:PSS (40 nm)/dendrimer (40 nm)/TPBI (30 nm)/LiF (1 nm)/Al (100 nm), in which ITO (indium tin oxide) and LiF/Al are the anode and cathode, respectively. PEDOT:PSS (poly(3,4-ethylenedioxythiophene):poly(styrene sulfonate)) acts as the hole-injecting and -transporting layer, TPBI (1,3,5-tris[N-(phenyl)benzimidazole]-benzene) as the electron-transporting and hole-blocking layer. Based on the good solubility and film-forming ability of these dendrimers, the emitting layers of the OLEDs were obtained by spin-coating the dendrimer solutions in chlorobenzene. The performance data are collected in Table 1. As shown by the EL spectra in Fig. 5, the **spiro-CN** based OLED exhibited blue electroluminescence with emission peaks at 422 and 448 nm, which is slightly red-shifted in comparison with the PL emission peak. The bathochromic effect in EL relative to the PL, which is frequently observed in OLEDs, should be ascribed to the additional influence of the electrical field on the excited state in OLEDs. The EL spectra show little change in position and profile with increasing driving voltage, indicating a relatively stable blue emission. The current density-voltage-brightness (J–V–B) characteristics and the EL efficiency curve of the **spiro-Cz** OLED are shown in Fig. 6. This device exhibited a maximum brightness of 287 cd/m^2 at 13 V and a maximum luminance efficiency of 0.35 cd/A. Similarly, the **spiro-CN** device emitted deep-blue electroluminescence at 412 nm with two shoulders at 448 and 480 nm (Fig. 7). This OLED exhibited a maximum brightness of 197 cd/m^2 at 11 V and a peak luminance efficiency of 0.47 cd/A. Although these EL performance data are not satisfied, the deep-blue electroluminescence and the extremely high glass transition temperature still indicate that these spirobifluorene-cored dendrimers are potential light-emitting materials for OLEDs application, especially for applications under high temperature.

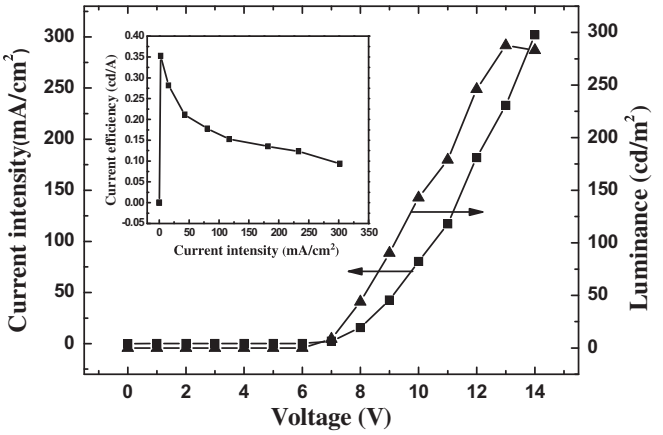

Fig. 6. The current density-voltage-brightness (J–V–B) characteristics of **spiro-Cz** OLED. Insert: the plot of current efficiency versus current density of the same device.

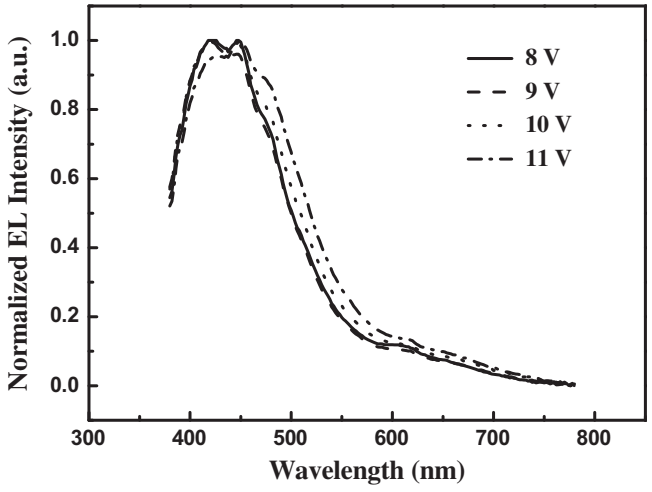

Fig. 5. The EL spectra of the **spiro-Cz** device under different voltages.

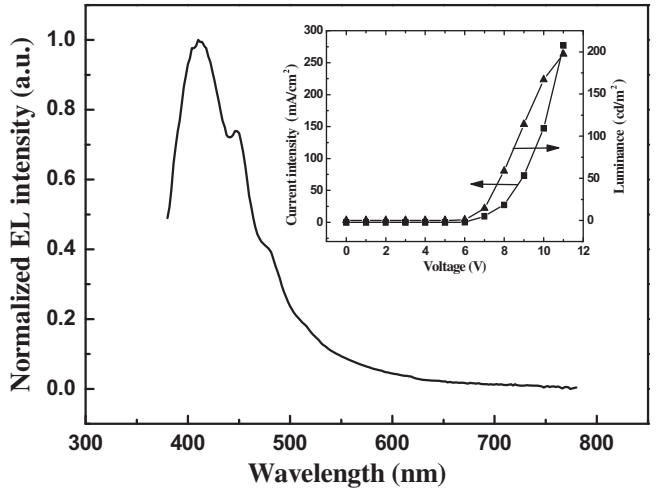

Fig. 7. The EL spectrum of **spiro-CN** OLED at 10 V. Insert: The current density-voltage-brightness (J–V–B) characteristics of the same device.

4. Conclusions

In summary, we have synthesized two novel spirobifluorene-cored dendrimers, **spiro-Cz** and **spiro-CN**, with polyphenylene dendrons and carbazole or cyano surface groups. **Spiro-Cz** is characterized by the amorphous nature even when it is obtained directly from organic solvents. An extremely high glass transition temperature of 332 °C was detected for **Spiro-Cz**, indicating a remarkable amorphous stability. Both dendrimers are also thermally stable and have good solubility in organic solvents. The absorption and fluorescence spectra of these dendrimers are almost identical to those in dilute solutions. All these good properties are suggested to benefit from the molecular design strategy by combining the spirobifluorene core and the bulky polyphenylene dendrons. The preliminary EL results of the devices made with these dendrimers demonstrate that they could be applied as active emitters in OLEDs.

Acknowledgments

We thank the National Natural Science Foundation of China (20704002) and the Fundamental Research Funds for the Central Universities (DUT10LK16) for financial support of this work.

References

[1] Bernius MT, Inbasekaran M, O'Brien J, Wu WS. Progress with light-emitting polymers. Adv Mater 2000;12:1737–50.
[2] Pei QB, Yang Y. Efficient photoluminescence and electroluminescence from a soluble polyfluorene. J Am Chem Soc 1996;118:7416–7.
[3] Li JY, Ziegler A, Wegner G. Substituent effect to prevent autoxidation and improve spectral stability in blue light-emitting polyfluorene. Chem Eur J 2005;11:4450–7.
[4] Lai WY, He QY, Zhu R, Chen QQ, Huang W. Kinked star-shaped fluorene//triazat- ruxene co-oligomer hybrids with enhanced functional properties for high-performance, solution-processed, blue organic light-emitting diodes. Adv Fun Mater 2008;18:265–76.
[5] Song S, Jin Y, Kim J, Park SH, Lee K, Suh H. A novel conjugated polymer based on cyclopenta[def] phenanthrene backbone with spiro group. Polymer 2008;49:5643–9.
[6] Saragi TPI, Spehr T, Siebert A, Fuhrmann-Lieker T, Salbeck J. Spiro compounds for organic optoelectronics. Chem Rev 2007;107:1011–65.
[7] Johansson N, Santos DA, Guo S, Cornil J, Fahlman M, Salbeck J, et al. Electronic structure and optical properties of electroluminescent spiro-type molecules. J Chem Phys 1997;107:2542–9.
[8] Wu CC, Lin YT, Chiang HH, Cho TY, Chen CW, Wong KT. Highly bright blue organic light-emitting devices using spirobifluorene-cored conjugated compounds. Appl Phys Lett 2002;81:577–9.
[9] Lee H, Oh J, Chu HY, Lee J, Kim SH, Yang YS, et al. Synthesis of region- and stereoselective alkoxy-substituted spirobifluorene derivatives for blue light emitting materials. Tetrahedron 2003;59:2773–9.
[10] Geng YH, Katsis D, Culligan SW, Ou JJ, Chen SW, Rothberg LJ. Fully spiro-configured terfluorenes as novel amorphous materials emitting blue light. Chem Mater 2002;14:463–70.
[11] Shen WJ, Dodda R, Wu CC, Wu FI, Liu TH, Chen HH, et al. Spirobifluorene-link bisanthracene: an efficient blue emitter with pronounced thermal stability. Chem Mater 2004;16:930–4.
[12] Pei J, Ni J, Zhou XH, Cao XY, Lai YH. Regioregular head-to-tail oligothiophene-functioalized 9,9′-spirobiflurene derivatives 2. NMR characterization, thermal behaviours, and electrochemical properties. J Org Chem 2002;67:8104–13.
[13] Lo SC, Burn PL. Development of dendrimers: macromolecules for use in organic light-emitting diodes and solar cells. Chem Rev 2007;107:1097–116.
[14] Li JY, Liu D. Dendrimers for organic light-emitting diodes. J Mater Chem 2009;19:7584–91.
[15] Pan J, Zhu W, Li S, Zeng W, Cao Y, Tian H. Dendron-functionalized perylene diimides with carrier-transporting ability for red luminescent materials. Polymer 2005;46:7658–69.
[16] Liu D, Ren H, Li J, Tao Q, Gao Z. Novel perylene bisimide derivative with fluorinated shell: a multifunctional material for use in optoelectronic devices. Chem Phys Lett 2009;482:72–6.
[17] Li SF, Zhong GY, Zhu WH, Li FY, Pan JF, Huang W, et al. Dendritic europium complex as a single dopant for white-light electroluminescent devices. J Mater Chem 2005;15:3221–8.
[18] Mitchell WJ, Kopidakis N, Rumbles G, Ginley DS, Shaheen SE. The synthesis and properties of solution processable phenyl cored thiophene dendrimers. J Mater Chem 2005;15:4518–28.
[19] Morgenroth F, Reuther E, Müllen K. Polyphenylene dendrimers: from three-dimensional to two-dimensional structures. Angew Chem Int Ed 1997;36:631–4.
[20] Thelakkat M, Schmidt HW. Synthesis and properties of novel derivatives of 1,3,5-tris(diarylamino)benzenes for electroluminescent devices. Adv Mater 1998;10:219–23.
[21] Rozwadowska MD. Cyanohydrins as substrates in benzoin condensation: regiocontrolled mixed benzoin condensation. Tetrahedron 1985;41:3135–40.
[22] Hamai S, Hirayama F. Actinometric determination of absolute fluorescence quantum yields. J Phys Chem 1983;87:83–9.
[23] Janietz S, Bradley DDC, Grell M, Giebeler C, Inbasekaran M, Woo EP. Electrochemical determination of the ionization potential and electron affinity of poly(9,9-dioctylfluorene). Appl Phys Lett 1998;73:2453–5.